Distributed Transient Safety Verification via Robust Control Invariant Sets: A Microgrid Application

Jean-Baptiste Bouvier[1,2], Sai Pushpak Nandanoori[1], Melkior Ornik[2] and Soumya Kundu[1]

***Abstract*— Modern safety-critical energy infrastructures are operated in a hierarchical and modular control framework allowing only limited data exchange between modules. In this context, to assure system-wide safety each module must synthesize and communicate constraints on the values of exchanged data. To ensure transient safety in inverter-based microgrids, we develop a set invariance-based distributed safety verification algorithm for each inverter module. Applying Nagumo's invariance condition, we construct a robust polynomial optimization problem to jointly search for safety-admissible set of control set-points and design parameters, under allowable disturbances from neighbors. We solve the verification problem with sum-of-squares programming and we perform numerical simulations using grid-forming inverters to illustrate our method.**

I. Introduction

Microgrids have shown promise to enhance power network reliability by coordinating distributed energy resources (DERs) as a locally operated entity [1]. However, ensuring operational stability, safety, and reliability of power networks is a complex multi-timescales problem, spanning subseconds to hours. Traditional methods decouple the slow and fast timescale to solve them separately, but the reduced inertia of inverter-based DERs is shrinking the timescale separation [2] and allows large variations of the voltage and frequency of each inverter [1], [3]. These changes occur during the transient evolution after a fault or in-between power set-points, and can lead to violation of safety constraints [4]. It is thus imperative to inform slower-timescale operations (e.g., optimal dispatch of power set-points) of the constraints arising from faster-timescale (transient) dynamics.

Many recent efforts have addressed this need via stability and security-constrained optimization [1], [3], or identification of parametric stability conditions [4]–[6]. However, most of the literature only focus on the stability, i.e., on the convergence of power system trajectories to its normal operating point. On the other hand, safety relates to avoiding critical operational limits (e.g., on voltages and frequencies), even under large disturbances. For instance, after an attack, the immediate priority is to contain the trajectories within some acceptable set, rather than ensuring return to normality.

[1]Jean-Baptiste Bouvier, Sai Pushpak Nandanoori and Soumya Kundu are with the Pacific Northwest National Laboratory, Richland, WA, USA. {saipushpak.n, soumya.kundu}@pnnl.gov

[2]Jean-Baptiste Bouvier and Melkior Ornik are with the Department of Aerospace Engineering and the Coordinated Science Laboratory at the University of Illinois Urbana-Champaign, Urbana, IL, USA. {bouvier3, mornik}@illinois.edu

Safety-constrained control techniques result in dynamic constraints over some prediction horizon, which are usually enforced with model-predictive control [7]. However, this method suffers from the nonlinearity of the power network dynamics, the information disparity due to communication overheads, and computational burden for long horizons [8]. To circumvent these issues, distributed safety verification methods based on robust forward set-invariance principles have been proposed in [8]–[10]. These prior works rely on the existence or the construction of parametric Lyapunov functions and/or barrier functions, thereby often incurring prohibitive computational costs and resulting in conservative safety certificates (Fig. 1 in [9]).

In this work, we consider a hierarchical and modular microgrid control architecture [10]–[12], which allows system-level dispatch of power set-points to inverter-based resources, accommodating only limited data exchange between the neighboring inverter modules. Our goal is to design bounds on control set-points at the inverter buses, that guarantee the safe excursions of local voltage and frequency within specified limits despite uncertainty in the neighboring buses. This work relies on the *Nagumo theorem* [13] to build an efficient method for distributed and robust safety verification, without using barrier functions. Thus, our approach requires less computation and is less conservative because the safe set is chosen by the user instead of being imposed by the barrier functions. The explicit reference governor [14] relies on the same concept but we establish safe bounds on control inputs, instead of deriving a control law, which is the role of the grid coordinator [10].

The main contributions of this article are threefold. Firstly, we determine the maximal bounds of the dispatched control set-points guaranteeing the safety of droop-controlled inverters. Secondly, we establish the monotonic relationship between this interval of safety admissible controls and the droop coefficients. Finally, we calculate efficiently the maximal droop coefficient for which these safety admissible controls exist. As such, this paper provides novel design guidelines for the droop coefficients, extending the literature on stability-informed droop settings, e.g., [4]–[6]. The remainder of this article is structured as follows. Section II provides a background of the relevant theory. Section III presents our microgrid problem of interest. Section IV explains our theoretical approach, illustrated on a numerical example in Section V using sum-of-squares programming.

II. Preliminaries

A. Invariant Sets

Consider a nonlinear dynamical system of the form

$$\dot{x}(t) = f\big(x(t)\big), \qquad x \in \mathbb{R}^n, \tag{1}$$

with f a Lipschitz continuous function. Our objective is to identify safe sets that the state x cannot leave. Such sets are called *invariant* (or *positively invariant*) in [13].

Definition 1: A set S is *invariant* by the dynamics (1) if $x(0) \in S$ yields $x(t) \in S$ for all $t \geq 0$.

To characterize these sets we use the Nagumo theorem [13].

Theorem 1 (Nagumo 1942): A closed set S is invariant by the dynamics (1) if and only if for all $x \in S$, $f(x) \in \mathcal{C}(x)$, with $\mathcal{C}(x)$ the Bouligand tangent cone to S at x.

A full definition of the Bouligand tangent cone is given in [13], but we will only be studying sets S where the Bouligand tangent cone is either $\mathbb{R}^+$ or $\mathbb{R}^-$. The geometrical interpretation of Nagumo's theorem is that f pointing inside S on its boundary prevents trajectories from leaving S.

B. Network Safety

In a network, the dynamics of node i can be modeled by

$$\dot{x}_i(t) = f_i(x_i, u_i, w_i),\ x_i \in \mathbb{R}^n,\ u_i(t) \in U,\ w_i(t) \in W, \tag{2}$$

with u_i a control input, w_i an external input, and U and W their respective admissible sets. For such a system we need to adapt our definition of invariant sets following [13].

Definition 2: A set S is *robust control invariant* by the dynamics (2) if there exists a feedback control law $u_i(t) \in U$ such that for all $x_i(0) \in S$ and all time-varying $w_i(t) \in W$, $x_i(t) \in S$ for all $t \geq 0$.

We then want to determine the set of control inputs u ensuring the robust control invariance of a given safe set S despite the fluctuations in the neighboring inverter states. In particular, specific to the example of inverter-based microgrids, i.e., when the safe sets are expressed as box constraints on the states (as in (5)), we define the following:

Definition 3: A 1-dimensional set $S = [\underline{s}, \overline{s}]$ is *upper invariant* (resp. *lower invariant*) for a set of controls U by the dynamics (2) if for all time-varying $w(t) \in W$, $u(t) \in U$ and all $x(0) \in S$, then $x(t) \leq \overline{s}$ $\big($resp. $x(t) \geq \underline{s}\big)$ for $t \geq 0$.

If S is upper invariant (resp. lower invariant), then the state cannot escape by crossing the upper bound (resp. lower bound) of S. Notice that if there are controls making S both upper and lower invariant, then S is a robust control invariant set. We denote such controls as *safety admissible*.

Definition 4: A set of controls U is *safety admissible* for the set S if for all controls $u(t) \in U$, the set S is robust control invariant.

III. Problem Description

A microgrid power network is operated by a microgrid coordinator that determines power setpoints for each node of the grid [10], [12]. The transition in between these setpoints, corresponding to a transient regime, might lead the frequency or voltage of some inverters to violate safety constraints. We are thus interested in ensuring the transient safety of microgrid networks, so that they are reliable when operated. Consider the case of droop-controlled inverters [4]:

$$\dot{\theta}_i = \omega_i, \tag{3a}$$

$$\tau_i \dot{\omega}_i = -\omega_i + \lambda_i^p \big(P_i^{set} - P_i\big), \tag{3b}$$

$$\tau_i \dot{v}_i = v_i^0 - v_i + \lambda_i^q \big(Q_i^{set} - Q_i\big), \tag{3c}$$

where θ_i, ω_i and v_i are, respectively, the phase angle, frequency and voltage magnitude of node i. The droop-coefficients $\lambda_i^p > 0$ and $\lambda_i^q > 0$ are associated with the active power vs. frequency and the reactive power vs. voltage droop curves, respectively. The time-constant of the low-pass filter used for the active and reactive power measurements is τ_i. The nominal voltage magnitude is v_i^0. The active power and reactive power set-points are P_i^{set} and Q_i^{set}, respectively. Finally, the active and reactive power P_i and Q_i follow the nonlinear coupling equations

$$P_i = v_i \sum_{k \in \mathcal{N}_i} v_k (G_{i,k} \cos\theta_{k,i} - B_{i,k} \sin\theta_{k,i}), \tag{4a}$$

$$Q_i = -v_i \sum_{k \in \mathcal{N}_i} v_k (G_{i,k} \sin\theta_{k,i} + B_{i,k} \cos\theta_{k,i}), \tag{4b}$$

where $\theta_{k,i} = \theta_k - \theta_i$, and $\mathcal{N}_i$ is the set of neighbor nodes with the convention that $i \in \mathcal{N}_i$. The transfer conductance and susceptance of the line connecting nodes i and k are denoted by $G_{i,k}$ and $B_{i,k}$, respectively.

We use the formulation of [9] to model the capability of the inverters to change their control set-points P_i^{set} and Q_i^{set} in order to adjust to different operating conditions as $P_i^{set} = P_i^0 + u_i^p$, and $Q_i^{set} = Q_i^0 + u_i^q$, where P_i^0 and Q_i^0 are the set-points for the nominal operating conditions; and u_i^p and u_i^q are control inputs. By a usual abuse of notation, instead of considering the actual voltage, we consider its difference from the nominal voltage $v_i^0 = 1$ p.u.. We are thus interested in maintaining at all times both voltage and frequency within some pre-specified safe sets. Following [9], [15], [16], we consider the safe sets to be

$$S_v = [\underline{v}, \overline{v}] = [-0.4, 0.2]\,\text{p.u.}\,, \tag{5a}$$

$$S_\omega = [\underline{\omega}, \overline{\omega}] = [-3, 3]\,\text{Hz}\,. \tag{5b}$$

For the inverters (3), the perturbation w_i from Definition 2 are the neighbor voltage magnitudes v_k and phase angle differences $\theta_{k,i}$. In (4) only the difference of θ_i and θ_k intervenes as opposed to their individual values, so without any loss of generality, we set $\theta_i \equiv 0$ as the *reference angle*, and use $\theta_{k,i} \equiv \theta_k$. Because microgrids are often characterized by relatively short lines between buses [17] we assume that the phase angle differences between neighbor buses are bounded: $\theta_k \in S_\theta = \big[-\frac{\pi}{6}, \frac{\pi}{6}\big]$ for all $k \in \mathcal{N}_i$.

Then, we want to determine controls $u_i = (u_i^p, u_i^q)$ that maintain $v_i \in S_v$ and $\omega_i \in S_\omega$, whatever the values of $\theta_k \in S_\theta$ and $v_k \in S_v$ for the neighbors $k \in \mathcal{N}_i$.

Problem 1: (Safety-Admissible Control) What values of control set-points u_i ensure that S_v and S_ω are robust control invariant by the dynamics (3)?

Moreover, note that the impact of neighbor disturbances on the inverter dynamics (3) are enhanced by larger droop values, which suggests the existence and size of the *safety-*

admissible controls depend on the chosen droop coefficients.

Problem 2: (Maximal Droop) What values of droop coefficients $(\lambda_i^p, \lambda_i^q)$ ensure the existence of a non-empty safety-admissible set of controls, guaranteeing robust control invariance of S_v and S_ω as per dynamics (3)?

IV. Theoretical Construction

We now establish the theory concerning robust control invariant sets for droop-controlled inverters. Since $\lambda_i^p > 0$ and $\lambda_i^q > 0$ in dynamics (3), we can define a *minimal lower control* $\underline{u}$ and a *maximal upper control* $\overline{u}$ such that

$$\underline{u} = \inf\big\{u_{low} \in \mathbb{R} : S \text{ is lower invariant for all } u \geq u_{low}\big\},$$
$$\overline{u} = \sup\big\{u_{up} \in \mathbb{R} : S \text{ is upper invariant for all } u \leq u_{up}\big\}.$$

If $\underline{u} \leq \overline{u}$, then the maximal interval of safety admissible controls is $[\underline{u}, \overline{u}]$. To illustrate these definitions and our objective let us study a simplified version of (3).

A. Simple Example

Consider dynamics (3b) with a single neighbor, $\tau = 1$s, $\lambda^p = 1$rad/s/p.u., $\theta_2 = 0$rad, $P^0 = 0$p.u., $G = -2$p.u.$^{-1}$ and a safe set $S = [-1, 1]$Hz. Then, $\dot{\omega} = -\omega + 2\omega\omega_2 + u$.

To make S upper invariant, according to Nagumo's theorem we need $\dot{\omega} \leq 0$ when $\omega = 1$. Thus, we want $2\omega_2 - 1 + u \leq 0$, so $u \leq 1 - 2\omega_2$ for all possible $\omega_2 \in S$. Then, the maximal upper control is $\overline{u} = -1$, because for $\omega_2 = 1$, we need $u \leq -1$.

Similarly, to make S lower invariant, we need $\dot{\omega} \geq 0$ when $\omega = -1$. Then, we want $-2\omega_2 + 1 + u \geq 0$, i.e., $u \geq -1 + 2\omega_2$. Thus, the minimal lower control is $\underline{u} = 1$.

Since $\overline{u} < \underline{u}$, there are no safety admissible controls making S robust control invariant. Indeed, λ^p is too large, to approximate (3b) with the stable dynamics $\tau_i\dot{\omega}_i = -\omega_i$.

B. Minimal controls for upper and lower invariance

Let us determine the minimal lower control for S_ω. By definition, $\underline{u_i^p} = \inf\limits_{\theta_k, v_k} \{u_i^p : \dot{\omega}_i \geq 0,\ \omega_i = \underline{\omega}\}$. With (3b), $\underline{u_i^p} = \inf\big\{u_i^p : u_i^p \geq \frac{1}{\lambda_i^p}\underline{\omega} + P_i - P_i^0,\ \forall \theta_k, v_k\big\}$. Then, the minimal u_i^p that is larger than all $\big[\frac{1}{\lambda_i^p}\underline{\omega} + P_i - P_i^0\big](\theta_k, v_k)$ is in fact the maximum of this term over all θ_k and v_k, because P_i is continuous in θ_k, v_k according to (4a) and, S_θ and S_v are compact. Thus,

$$\begin{aligned} \underline{u_i^p} = \max_{\theta_k, v_k}\ & \frac{1}{\lambda_i^p}\underline{\omega} + P_i - P_i^0, \\ \text{subject to}\quad & \theta_k \in S_\theta,\ v_k \in S_v,\ k \in \mathcal{N}_i. \end{aligned} \tag{6}$$

Then, $\dot{\omega}_i \geq 0$ when $\omega_i = \underline{\omega}$ and $u_i^p \geq \underline{u_i^p}$ for all $\theta \in S_\theta$ and $v \in S_v$, which guarantees lower invariance according to Nagumo's theorem. Similarly, the maximal upper control is

$$\begin{aligned} \overline{u_i^p} = \min_{\theta_k, v_k}\ & \frac{1}{\lambda_i^p}\overline{\omega} + P_i - P_i^0, \\ \text{subject to}\quad & \theta_k \in S_\theta,\ v_k \in S_v,\ k \in \mathcal{N}_i, \end{aligned} \tag{7}$$

and makes $\dot{\omega}_i \leq 0$ when $\omega_i = \overline{\omega}$ and $u_i^p \leq \overline{u_i^p}$ for all $\theta \in S_\theta$ and $v \in S_v$. The minimal lower control $\underline{u_i^q}$ and maximal upper control $\overline{u_i^q}$ for (3c) are defined similarly.

A great way to solve the optimization problems (6) and (7) is to use a sum-of-squares (SOS) optimization. A multivariate polynomial $p(x)$, $x \in \mathbb{R}^n$, is an SOS if there exist polynomial functions $h_i(x)$, $i = 1, \ldots, s$ such that $p(x) = \sum_{i=1}^s h_i^2(x)$. However, the power-flow equations (4) are not polynomials. Following [9] we choose a third order Taylor expansion of the dynamics (4) to make (3) polynomial. Then, (6) and (7) can be solved with any SOS tool.

C. Maximal droop for robust control invariance

The stability of the voltage and frequency rely on small droop coefficients λ. As in Section IV-A, when λ increases in (3), the perturbations P and Q increase, and thus the set of safety admissible controls should shrink. Because the optimizations in (6) and (7) only affect P_i, we introduce the maximum and minimum of the active and reactive powers (4) at the lower and upper bounds of S_ω and S_v

$$\begin{aligned} P_i^{max} &= \max\big\{P_i : \omega_i = \underline{\omega},\ (\theta_k, v_k) \in S_\theta \times S_v,\ k \in \mathcal{N}_i\big\}, \\ P_i^{min} &= \min\big\{P_i : \omega_i = \overline{\omega},\ (\theta_k, v_k) \in S_\theta \times S_v,\ k \in \mathcal{N}_i\big\}, \\ Q_i^{max} &= \max\big\{Q_i : v_i = \underline{v},\ (\theta_k, v_k) \in S_\theta \times S_v,\ k \in \mathcal{N}_i\big\}, \\ Q_i^{min} &= \min\big\{Q_i : v_i = \overline{v},\ (\theta_k, v_k) \in S_\theta \times S_v,\ k \in \mathcal{N}_i\big\}. \end{aligned}$$

Proposition 1: The bounds of the interval of safety admissible controls $[\underline{u}, \overline{u}]$ for S_v and S_ω are inversely proportional to the droop coefficient λ.

Proof: With the above definitions, (6) and (7) yield

$$\underline{u_i^p}(\lambda_i^p) = \frac{\underline{\omega}}{\lambda_i^p} + P_i^{max} - P_i^0,\ \overline{u_i^p}(\lambda_i^p) = \frac{\overline{\omega}}{\lambda_i^p} + P_i^{min} - P_i^0. \tag{8}$$

A similar result holds for the voltage. ∎

Building on this result, we can then establish a sufficient condition for the existence of safety admissible controls.

Proposition 2: If the safe set contains 0 in its interior, then safety admissible controls exist for some droop coefficients.

Proof: Because ω_i does not intervene in P_i (4a), the constraints for P_i^{min} and P_i^{max} are the same, which leads to $P_i^{min} < P_i^{max}$. Then, based on (8), the condition $\underline{\omega} < 0 < \overline{\omega}$ is necessary and sufficient to make $\underline{u_i^p}(\lambda_i^p) < \overline{u_i^p}(\lambda_i^p)$ for λ_i^p small enough. On the other hand, since v_i intervenes in Q_i (4b), we cannot order Q_i^{min} and Q_i^{max} without computing them. Thus the condition $\underline{v} < 0 < \overline{v}$ is sufficient but maybe not necessary to make $\underline{u_i^q}(\lambda_i^q) < \overline{u_i^q}(\lambda_i^q)$ for some λ_i^q. ∎

Then, the safe sets of (5) guarantee that safety admissible controls exist for some small enough droop coefficients. We now want to find the maximal droop coefficient λ^* for which safety admissible controls exist, i.e.,

$$\lambda^* = \max\big\{\lambda \geq 0 : \underline{u}(\lambda) \leq \overline{u}(\lambda)\big\}. \tag{9}$$

Remark 1: Note that the problem of identifying the maximal droop for stability analysis is relatively well studied in the literature (see, for instance, [4]–[6]). However, as a novel contribution of this paper, we propose a method to identify maximal droop values for safety verification.

According to Proposition 1 and 2, if 0 is in the interior of S and $\lambda \leq \lambda^*$, then the interval $[\underline{u}(\lambda), \overline{u}(\lambda)]$ is not empty, is proportional with $1/\lambda$ and makes S robust control invariant,.

Proposition 3: The maximal droop coefficient λ^* is

$$\lambda_i^{p*} = \frac{\overline{\omega} - \underline{\omega}}{P_i^{max} - P_i^{min}} \quad \text{and} \quad \lambda_i^{q*} = \frac{\overline{v} - \underline{v}}{Q_i^{max} - Q_i^{min}}. \tag{10}$$

Proof: Since $\underline{u_i^p}$ and $\overline{u_i^p}$ are continuous in λ_i^p according to (8), definition (9) leads to $\underline{u_i^p}(\lambda_i^{p*}) = \overline{u_i^p}(\lambda_i^{p*})$. Using (8) we easily obtain the announced expression for λ_i^{p*}. The calculation of λ_i^{q*} is similar. ∎

The term $P^{max} - P^{min}$ in the denominator validates our intuition that increasing the range of possible perturbations decreases λ^{p*}. The larger $\overline{\omega} - \underline{\omega}$ is, the larger ω can be, and thus the stronger the stabilizing term $-\omega$ is in (3b), which increases λ^{p*}. The same analysis holds for λ^{q*}.

Remark 2: There are now two approaches to answer Problem 1 based on the controls $\underline{u}$ and $\overline{u}$. If $\lambda \leq \lambda^*$, then $\underline{u} \leq \overline{u}$ and any control in between guarantees the robust control invariance of the safe set. On the other hand, if $\lambda > \lambda^*$ we need a state-dependent control law. When the state gets too close from the upper (resp. lower) bound of its safe set, applying $\overline{u}$ (resp. $\underline{u}$) prevents safety violation. Besides, $\underline{u}$ and $\overline{u}$ can be precomputed, so that the sole real-time action of the controller is to decide which one of the controls to apply.

V. Numerical Analysis

In this section we apply our theory to a modified microgrid model [18], and demonstrate the robust control invariance of the safe sets S_v and S_ω introduced in (5). As per the modifications in [9], [10], four inverters were placed in the network, three of those at buses $1, 4$, and 5, and the fourth at bus 0 after disconnecting the utility for islanded operation.

In a microgrid, the distance between inverters is small and thus the states of neighbors are strongly coupled. To account for this physical phenomenon we introduce two constants Δ_v and Δ_ω measuring the range of allowable uncertainty of neighboring inverters such that $v_k \in [v_i - \Delta_v, v_i + \Delta_v]$ and $\omega_k \in [\omega_i - \Delta_\omega, \omega_i + \Delta_\omega]$ for $k \in \mathcal{N}_i$. For the numerical analysis we choose $\Delta_v = 0.02$p.u., which is 2% of the nominal voltage v_i^0, and $\Delta_\omega = 0.12$Hz, which is 2% of the 6Hz range of S_ω. The nominal droop coefficients of the network are $\lambda^p = 2.51$rad/s/p.u. and $\lambda^q = 0.2$p.u./p.u..

The coupling adds a constraint to the calculation of Q_i^{min} and Q_i^{max}. For instance, $Q_i^{max} = \max\ Q_i(\theta_k, v_k)$ subject to $v_i = \underline{v}$, $\theta_k \in S_\theta$, $v_k \in S_v \cap [v_i - \Delta_v, v_i + \Delta_v] = [\underline{v}, \underline{v} + \Delta_v]$ for $k \in \mathcal{N}_i$. We compute Q_2^{min}, Q_2^{max} with an SOS algorithm and we use Proposition 1 to represent $\underline{u_2^q}$ and $\overline{u_2^q}$ on Fig. 1.

Fig. 1: Evolution of the interval of safety admissible controls in blue for the voltage of node 2. The blue dot corresponds to λ_2^{q*}. The green dash-dot lines correspond to $\underline{u_2^q}(\lambda_2^q)$ and $\overline{u_2^q}(\lambda_2^q)$. The red dotted line indicates that $\underline{u_2^q} > \overline{u_2^q}$.

As proven in Proposition 2, since 0 is in the interior of S_v, we were able to find values of λ_2^q for which safety admissible controls exist. On Fig. 1, λ_2^{q*} is located at the intersection of the green dash-dot lines representing $\underline{u_2^q}(\lambda_2^q)$ and $\overline{u_2^q}(\lambda_2^q)$. Fig. 2 shows that the same is true for λ_2^p.

Fig. 2: Evolution of the interval of safety admissible controls in blue for the frequency of node 2. The blue dot corresponds to λ_2^{p*}. The green dash-dot lines correspond to $\underline{u_2^p}(\lambda_2^p)$ and $\overline{u_2^p}(\lambda_2^p)$. The red dotted line indicates that $\underline{u_2^p} > \overline{u_2^p}$.

The computed values of λ^* are gathered in Table I.

Inverter	1	2	3	4
λ^{p*} [rad/s/p.u.]	1.227	2.329	0.875	1.368
λ^{q*} [p.u./p.u.]	0.228	0.434	0.161	0.241

TABLE I: Maximal droop coefficients λ^* for which safety admissible controls exist.

Note that for the voltage λ^{q*} ranges from 80% to 217% of the nominal λ^q depending on the inverter. For the frequency, λ^{p*} ranges from 35% to 93% of the nominal λ^p. We now study how the admissible range of states Δ_v, S_θ and S_v impact the maximal droop coefficient λ^{q*}.

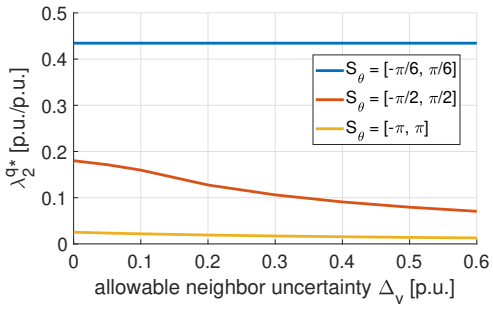

Fig. 3: The effect of allowable neighbor uncertainty Δ_v and of the range of admissible phase angle S_θ on λ_2^{q*}.

In Figures 3 and 4, $\Delta_v = 0.6$p.u. depicts a lack of coupling between inverters, because the length of S_v is at most 0.6p.u., while for $\Delta_v = 0$p.u. the coupling is perfect, i.e., $v_k = v_i$ for $k \in \mathcal{N}_i$.

As predicted with (10) and illustrated on Figures 3 and 4, as the uncertainty ranges Δ_v and S_θ increase, the value of λ^{q*} decreases. The impact of the length of S_v on λ^{q*} is more difficult to predict as it affects both the numerator and denominator of λ^{q*} in (10). However, the verdict of Fig. 4 is clear: enlarging S_v increases λ^{q*}, the voltage has more room inside its safe set, it is thus easier to keep $v \in S_v$.

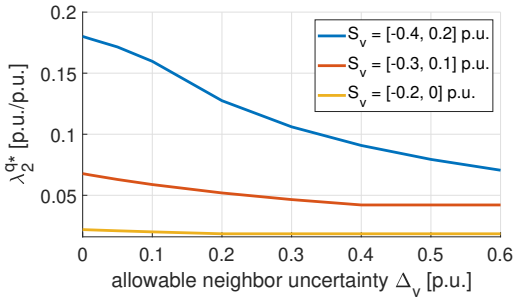

Fig. 4: The effect of allowable neighbor uncertainty Δ_v and of the range of admissible phase angle S_v on λ_2^{q*}.

We compute the controls u_1^p and $\overline{u_1^p}$ on an Intel Core i7-4770S with a CPU at 3.1GHz and 8GB of RAM. Previous works [5], [9] relied on the widely used MATLAB toolbox SOSTOOLS and the semi-definite programming (SDP) solver SeDuMi. However, the computation times were often excessive for nodes with more than two neighbors. As an illustration, we computed u_1^p and $\overline{u_1^p}$ in MATLAB with SeDuMi in 4295s, while using the Julia language and the SDP solvers SDPA and Mosek reduced the computation times to only 343s and 33s respectively.

In order to illustrate the invariance of the safe sets with the safety admissible controls calculated, we simulate the evolution of the voltage and the frequency of node 1. We use the original non-polynomial dynamics of the system. We choose λ_1^p and λ_1^q at respectively 40% and 100% of their nominal values, so that $\lambda_1^p < \lambda_1^{p*}$ and $\lambda_1^q < \lambda_1^{q*}$. Then, the intervals of safety admissible controls are $U_\omega = [-0.724, 1.571]$p.u. and $U_v = [-0.25, -0.0937]$p.u..

Every second we randomly choose control values $u_1^q \in U_v$ and $u_1^p \in U_\omega$ as shown on Figures 5(a) and 5(b). Similarly, the states $\omega_k \in S_\omega \cap [\omega_1 - \Delta_\omega, \omega_1 + \Delta_\omega]$ and $v_k \in S_v \cap [v_1 - \Delta_v, v_1 + \Delta_v]$ of the neighboring nodes are stochastically updated every 10ms as depicted on Figures 5(c) and 5(d). The evolution of the voltage and frequency of node 1 are then pictured on Figures 5(e) and 5(f).

We can see that even randomly chosen controls, as long as they are within the safety admissible interval, enforce the safety of the system as $v_1 \in S_v$ and $\omega_1 \in S_\omega$ despite the stochastic variations of the neighbor states.

One could rightfully object that the stochastic nature of the variations of the neighbor states ω_k and v_k prevent significant changes in v_1 and ω_1 that could lead to safety violations. To overcome this limitation, we run a similar simulation where the neighbor states take their worst case values. To keep a constant phase angle $\theta_k = -\frac{\pi}{6}$rad, we need a constant frequency $\omega_k = 0$Hz and thus the frequency coupling must be removed by taking $\Delta_\omega = \infty$. We set the voltage at its lowest admissible bound, i.e., $v_k = \max\{\underline{v}, v_i - \Delta_v\}$. We keep the same stochastic controls and same droop values.

Fig. 6(a) shows how the voltage of a neighboring inverter v_3 follows its admissible lower bound. As illustrated on Fig. 6(b) and 6(c) the voltage v_1 is maintained in S_v and the frequency ω_1 is maintained in S_ω despite the stochastic safety admissible controls and the lower bound neighbor states. Similar results are obtained when choosing θ_k at its upper bound $\frac{\pi}{6}$ and/or v_k at its upper bound $\min\{\overline{v}, v_i + \Delta_v\}$.

VI. Conclusion and Future Work

In this paper we considered the problem of transient safety in inverter-based microgrids. Relying on Nagumo's theorem, we developed two approaches to enforce the invariance of frequency and voltage sets of droop-controlled inverters. We solved the resulting optimization problems with SOS algorithms and successfully illustrated the safety methods on a microgrid model.

There are three promising avenues of future work. We first want to compare the efficiency of our approach in terms of size of invariant set and of computation times with barrier function and explicit governor approaches. We believe that a similar method can be used to handle safe energy storage, with only adding a state of charge constraint to the problem. Finally, we want to demonstrate our approach in conjunction with system level optimal dispatch problem.

Acknowledgment

This research was supported by the Resilience through Data-driven Intelligently-Designed Control Initiative, under the Laboratory Directed Research and Development Program at Pacific Northwest National Laboratory (PNNL). PNNL is a multi-program national laboratory operated for the U.S. Department of Energy by Battelle Memorial Institute under Contract No. DE-AC05-76RL01830.

References

[1] Y. Xu, C.-C. Liu, K. P. Schneider, F. K. Tuffner, and D. T. Ton, "Microgrids for service restoration to critical load in a resilient distribution system," *IEEE Transactions on Smart Grid*, vol. 9, no. 1, pp. 426 – 437, 2016.

[2] J. A. Taylor, S. V. Dhople, and D. S. Callaway, "Power systems without fuel," *Renewable and Sustainable Energy Reviews*, vol. 57, pp. 1322 – 1336, 2016.

[3] A. Maulik and D. Das, "Stability constrained economic operation of islanded droop-controlled DC microgrids," *IEEE Transactions on Sustainable Energy*, vol. 10, no. 2, pp. 569 – 578, 2018.

[4] J. Schiffer, R. Ortega, A. Astolfi, J. Raisch, and T. Sezi, "Conditions for stability of droop-controlled inverter-based microgrids," *Automatica*, vol. 50, no. 10, pp. 2457 – 2469, 2014.

[5] S. Kundu, W. Du, S. P. Nandanoori, F. Tuffner, and K. Schneider, "Identifying parameter space for robust stability in nonlinear networks: A microgrid application," in *American Control Conference*. IEEE, 2019, pp. 3111 – 3116.

[6] S. P. Nandanoori, S. Kundu, W. Du, F. K. Tuffner, and K. P. Schneider, "Distributed small-signal stability conditions for inverter-based unbalanced microgrids," *IEEE Transactions on Power Systems*, vol. 35, no. 5, pp. 3981 – 3990, 2020.

[7] D. Q. Mayne, J. B. Rawlings, C. V. Rao, and P. O. Scokaert, "Constrained model predictive control: Stability and optimality," *Automatica*, vol. 36, no. 6, pp. 789–814, 2000.

[8] Y. Zhang and J. Cortés, "Distributed bilayered control for transient frequency safety and system stability in power grids," *IEEE Transactions on Control of Network Systems*, vol. 7, no. 3, pp. 1476–1488, 2020.

[9] S. Kundu, S. Geng, S. P. Nandanoori, I. A. Hiskens, and K. Kalsi, "Distributed barrier certificates for safe operation of inverter-based microgrids," in *American Control Conference*. IEEE, 2019, pp. 1042 – 1047.

[10] S. Kundu and K. Kalsi, "Transient safety filter design for grid-forming inverters," in *American Control Conference*. IEEE, 2020, pp. 1299 – 1304.

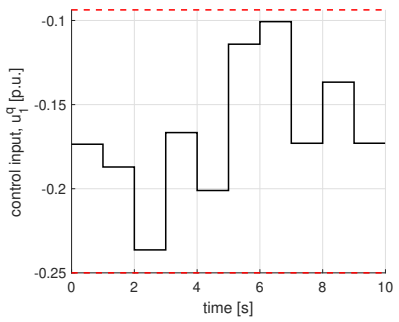

(a) Stochastic choice of $u_1^q \in U_v$, where U_v is the interval of safety admissible controls.

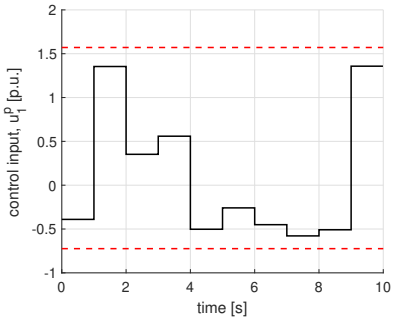

(b) Stochastic choice of $u_1^p \in U_\omega$, where U_ω is the interval of safety admissible controls.

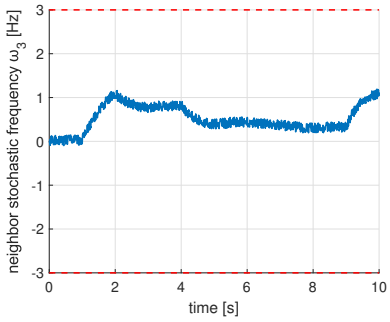

(c) Stochastic choice of neighbor frequency $\omega_3 \in S_\omega \cap [\omega_1 - \Delta_\omega, \omega_1 + \Delta_\omega]$.

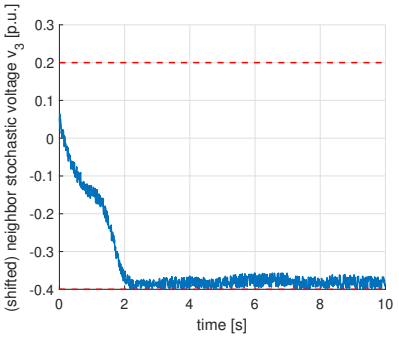

(d) Stochastic choice of neighbor voltage $v_3 \in S_v \cap [v_1 - \Delta_v, v_1 + \Delta_v]$.

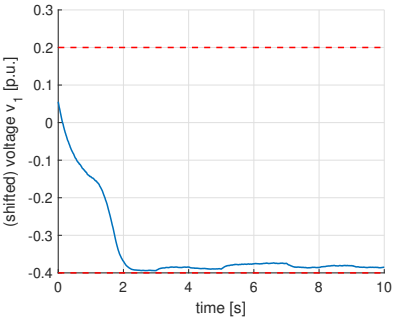

(e) Evolution of v_1, kept in S_v by u_1^q.

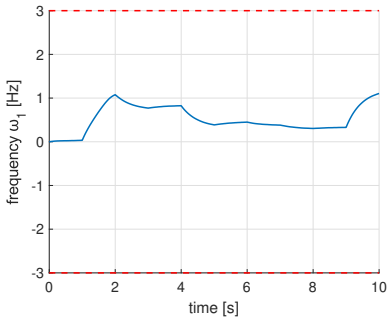

(f) Evolution of ω_1, kept in S_ω by u_1^p.

Fig. 5: Simulation of the voltage v_1 and frequency ω_1 under stochastic safety admissible controls u_1^q and u_1^p, and stochastic variations of neighbor states θ_2, θ_3, v_2 and v_3.

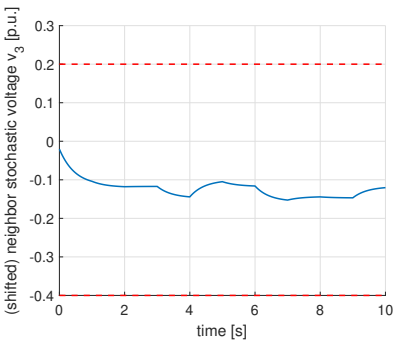

(a) Evolution of $v_3 = \max\{\underline{v}, v_i - \Delta_v\}$.

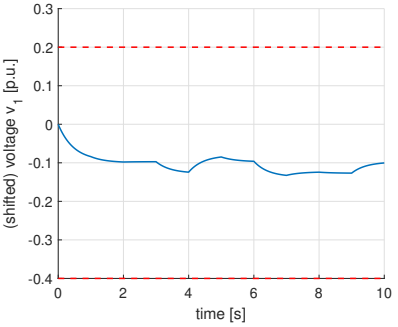

(b) Evolution of v_1, kept in S_v by u_1^q.

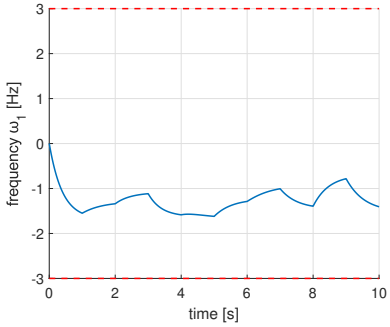

(c) Evolution of ω_1, kept in S_ω by u_1^p.

Fig. 6: Simulation of the voltage v_1 and frequency ω_1 under stochastic safety admissible controls u_1^q and u_1^p, and lower bound choice of neighbor states θ_2, θ_3, v_2 and v_3.

[11] J. M. Guerrero, J. C. Vasquez, J. Matas, L. G. De Vicuña, and M. Castilla, "Hierarchical control of droop-controlled ac and dc microgrids—a general approach toward standardization," *IEEE Transactions on Industrial Electronics*, vol. 58, no. 1, pp. 158–172, 2010.

[12] M. Almassalkhi, S. Brahma, N. Nazir, H. Ossareh, P. Racherla, S. Kundu, S. P. Nandanoori, T. Ramachandran, A. Singhal, D. Gayme *et al.*, "Hierarchical, grid-aware, and economically optimal coordination of distributed energy resources in realistic distribution systems," *Energies*, vol. 13, no. 23, p. 6399, 2020.

[13] F. Blanchini, "Set invariance in control," *Automatica*, vol. 35, no. 11, pp. 1747 – 1767, 1999.

[14] M. M. Nicotra and E. Garone, "The explicit reference governor: A general framework for the closed-form control of constrained nonlinear systems," *IEEE Control Systems Magazine*, vol. 38, no. 4, pp. 89–107, 2018.

[15] K. P. Schneider, N. Radhakrishnan, Y. Tang, F. K. Tuffner, C.-C. Liu, J. Xie, and D. Ton, "Improving primary frequency response to support networked microgrid operations," *IEEE Transactions on Power Systems*, vol. 34, no. 1, pp. 659 – 667, 2018.

[16] J. Elizondo, R. Y. Zhang, P.-H. Huang, J. K. White, and J. L. Kirtley, "Inertial and frequency response of microgrids with induction motors," in *17th Workshop on Control and Modeling for Power Electronics*. IEEE, 2016, pp. 1 – 6.

[17] W. H. Kersting, "Radial distribution test feeders," *IEEE Transactions on Power Systems*, vol. 6, no. 3, pp. 975–985, 1991.

[18] T. Ersal, C. Ahn, I. A. Hiskens, H. Peng, and J. L. Stein, "Impact of controlled plug-in evs on microgrids: A military microgrid example," in *Power and Energy Society General Meeting*. IEEE, 2011, pp. 1–7.